

# Mechanochemical Activation of Solid Salts $K_2PtX_6$ ( $X = Cl, Br$ )

S. A. Mitchenko<sup>1,2</sup>, E. V. Khomutov<sup>2</sup>, V. V. Kovalenko<sup>2</sup>, and I. P. Beletskaya<sup>3</sup>

<sup>1</sup> *Nesmeyanov Institute of Organoelement Compounds, Russian Academy of Sciences, Moscow, 117813 Russia*

<sup>2</sup> *Litvinenko Institute of Physicoorganic and Coal Chemistry, National Academy of Sciences of Ukraine, Donetsk, 340114 Ukraine*

<sup>3</sup> *Department of Chemistry, Moscow State University, Moscow, 117234 Russia*

Received May 22, 2001

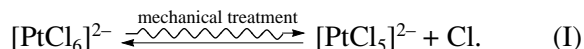
**Abstract**—Mechanochemical treatment of solid-phase  $K_2PtX_6$  salts in a vibrating mill in an argon or air atmosphere produced paramagnetic Pt(III) complexes via the homolytic cleavage of the Pt–X bond. Lewis acid sites were found on the surface of the mechanically activated  $K_2PtCl_6$  salt using the paramagnetic probe method. The sites can be attributed to coordinatively unsaturated Pt(IV) complexes formed via Pt–Cl bond heterolysis.

## INTRODUCTION

Platinum(II) and platinum(III) acidic complexes in aqueous and methanol solutions catalyze several transformations of different hydrocarbons and their derivatives. The Pt(II) chloride complexes catalyze the functionalization of saturated and aromatic hydrocarbons [1–3]. The Pt(II) iodide complexes catalyze ethylene hydroiodination to ethyl iodide [4]. The Pt(IV) iodide complexes in acidic solutions catalyze acetylene hydroiodination to vinyl iodide [5], whereas in neutral solutions they catalyze acetylene dimerization accompanied by iodine addition to form (*E,E*)-1,4-diiodobutadiene-1,3 [6]. The silica-supported platinum chloride complexes activate alkanes [7]. Nontraditional methods for the preparation of heterogeneous catalysts, including mechanochemical treatment, have been intensively developed in recent years [8–10]. In this connection, the study of the transformations of platinum halide complexes under the mechanical treatment of the solid-phase  $K_2PtCl_6$  and  $K_2PtCl_4$  salts is of interest.

It is known that the mechanical treatment of covalent crystals, such as diamond, graphite, silicon, silica, and others, in mills where mechanical destruction is accompanied by the friction of particles results in the cleavage of chemical bonds between species localized in the sites of the crystalline lattice and generates free radicals [11]. The mechanical treatment of ionic crystals of the magnesium oxide type in the friction regime also results in the transfer of an electron from an anionic site to a cationic site of the lattice to form reactive radical ion pairs [11]  $\{Mg^{2+}O^{2-}\} \longrightarrow \{Mg^{+}\cdot O^{-}\}$ . We found [12] that the mechanical treatment of the solid-phase  $K_2PtX_6$  ( $X = Cl, Br$ ) salts with the ion-crystalline structure in which the anionic site was occupied by the  $[PtX_6]^{2-}$  complex ion also resulted in the cleav-

age of chemical bonds but between species composing the anionic site



The purpose of this work is the detailed ESR study of the mechanically activated transformations in the coordination sphere of the Pt(IV) halide complexes.

## EXPERIMENTAL

Samples were activated in an MMVE-0.005 micro-mill for 1 h at room temperature in air<sup>1</sup> using a closed glass vibrating reactor containing glass grinding bodies. The working frequency and the amplitude of vibrations of the vibrating reactor were  $f = 50$  Hz and  $h_0 = 5.5$  mm, respectively, which corresponded to a specific rating of  $\sim 15$  W/kg.

The  $K_2PtX_6$  and  $K_2PtX_4$  ( $X = Cl, Br$ ) salts were prepared using a standard procedure [13] and thoroughly dried. All procedures with the salts were carried out in a dry box.

Measurements were conducted with an SE/X-2544 microwave spectrometer with a working frequency of 9.4 GHz. The magnetic field was calibrated by a nuclear magnetometer. The Mn(II) sample in the MgO matrix was used as a standard. ESR spectra were recorded in solid polycrystalline samples at room temperature and 77 K.

2,2,6,6-Tetramethylpiperidin-1-oxyl (TEMPO) was used as a paramagnetic probe. An aliquot (0.6 ml) of a solution of the nitroxyl radical ( $2 \times 10^{-3}$  mol/l) in hexane was injected with a syringe through a rubber gasket into the vibrating reactor filled with the activated platinum salt, after which the solvent was evaporated in an argon flow.

<sup>1</sup> Independent experiments showed that the reactions also occurred in argon.

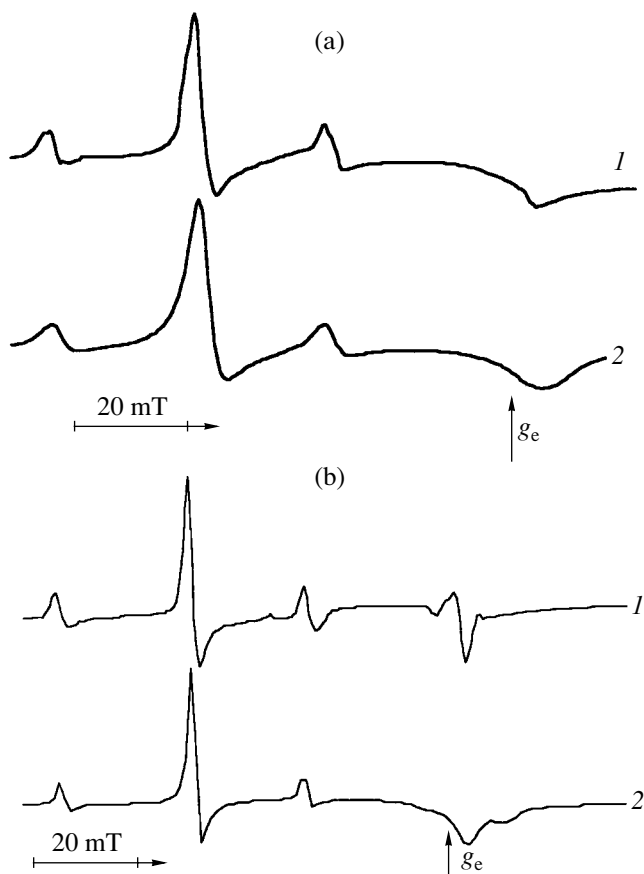


**Fig. 1.** (1) Detected and (2) theoretical ESR spectra of the  $\text{Pt}^{3+}$  complexes produced by the mechanical treatment of the  $\text{K}_2\text{PtCl}_6 + \text{K}_2\text{PtCl}_4$  mixture at (a) room temperature and (b) 77 K.

The accumulation of methyl chloride in the reaction of methyl iodide was monitored by chromatography as described in [4].

## RESULTS AND DISCUSSION

The addition of  $\text{MeI}$  vapor to the reactor after the mechanical treatment of  $\text{K}_2\text{PtCl}_6$  results in the almost instant formation of methyl chloride. The latter is not formed if before the addition of methyl iodide the reactor with the freshly activated  $\text{K}_2\text{PtCl}_6$  salt was purged with dry argon. Since in the gas phase methyl iodide rapidly reacts with  $\text{Cl}_2$  to form methyl chloride, these facts can be explained by the accumulation of chlorine in the closed reactor during the treatment of  $\text{K}_2\text{PtCl}_6$ . It is known that these reactions of oxidative nucleophilic substitution of iodide in alkyl iodides, which were first observed in 1905 [15], readily occur under the action of such oxidants as  $\text{Cl}_2$  and  $\text{Br}_2$  [16]. However, it is impossible to determine the amount of evolved chlorine because of its partial tribosorption [17] into a  $\text{K}_2\text{PtCl}_6$  matrix.

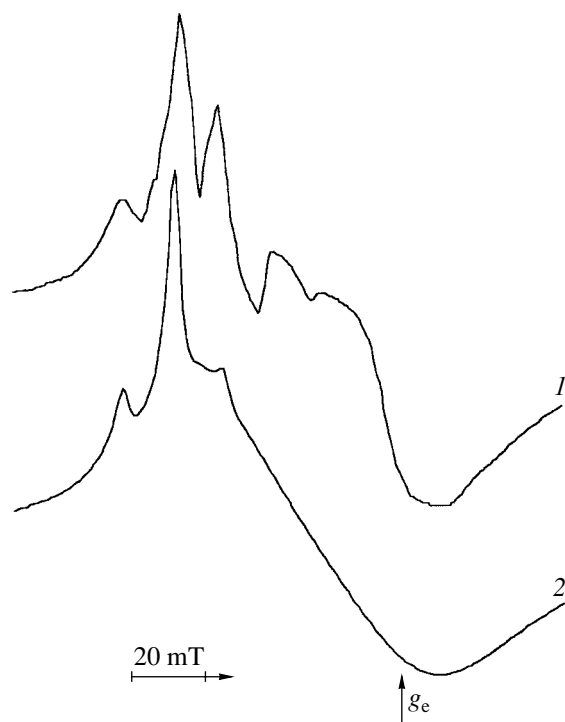


**Fig. 2.** ESR spectrum of the  $\text{Pt}^{3+}$  complexes produced by the mechanical treatment of the  $\text{K}_2\text{PtBr}_6 + \text{K}_2\text{PtBr}_4$  mixture: (1) experimental and (2) theoretical spectra at room temperature.

The mechanochemical treatment of the  $\text{K}_2\text{PtCl}_6$  complex salt also results in the appearance of a relatively weak ESR signal with the resolved hyperfine structure (HFS) from the  $^{195}\text{Pt}$  nuclei (Fig. 1). More intense signals (see below) are observed in the samples obtained by the grinding of  $\text{K}_2\text{PtCl}_6$  powder containing minor additives of  $\text{K}_2\text{PtCl}_4$  (5–15 mol %). The mechanical activation of  $\text{K}_2\text{PtCl}_6$  in a  $\text{Cl}_2$  atmosphere does not produce this signal in the ESR spectrum. Similar effects are observed for the treatment of the  $\text{K}_2\text{PtBr}_6 + \text{K}_2\text{PtBr}_4$  mixture (Fig. 2). The ESR spectrum of  $\text{Pt}^{3+}$ , which is obtained by the grinding of the  $\text{K}_2\text{PtCl}_6$  powder with the  $\text{K}_2\text{PtBr}_4$  additive (15 mol %), is a superposition of a more intense signal from platinum(III) chloride and a weak signal from platinum(III) bromide (Fig. 3).

The spectra (Figs. 1 and 2) correspond to the axially symmetric spin Hamiltonian

$$H = g_{\parallel}\beta H_z S_z + g_{\perp}\beta(H_x S_x + H_y S_y) + A_{\parallel} S_z I_z + A_{\perp} (S_x I_x + S_y I_y), \quad (1)$$

where  $S = 1/2$  is the electron spin,  $I = 1/2$  is the spin of the magnetic platinum isotope, and  $\beta$  is Bohr's magneton. The other parameters are presented in the table, which also contains the parameters of ESR spectra for some other Pt(III) compounds characterized by the axially symmetric spin Hamiltonian for comparison. Theoretical ESR spectra for the axial symmetry were plot-

ted for the more exact determination of the spin Hamiltonian parameters (Figs. 1 and 2). The  $g$  factor and hyperfine interaction (HFI) constants were taken into account in the framework of second-order perturbation theory. Good coincidence of theoretical and experimental spectra confirms that the lines were correctly assigned, and the presence of the HFS from the  $^{195}\text{Pt}$  isotope in the perpendicular orientation proves that the spectrum belongs to the Pt(III) compound. When the samples are cooled to 77 K, the lines become narrower (Fig. 1b), which is evidently a consequence of the temperature function of the characteristic time of spin-lattice relaxation. However, at 77 K the HFS from the magnetic platinum isotope nucleus in the parallel orientation was not observed either. Therefore, the  $A_{\parallel}$  HFC constant must be lower than the line width. This gives  $A_{\parallel}$  of  $(0 \pm 35) \times 10^{-4} \text{ cm}^{-1}$  at 77 K and  $<65 \times 10^{-4} \text{ cm}^{-1}$  at room temperature. Let us compare the spectral parameters of different Pt(III) compounds with the axially symmetric spin Hamiltonian (see table). For these complexes,  $g_{\parallel}$  are close to two, and  $g_{\perp}$  are much higher than two. The axial character of symmetry of the spectra and the  $g$  factor values indicate [19, 20] the localization of an unpaired electron predominantly on the  $5d_{z^2}$  orbital and, hence, the square-pyramidal structure of the complex. The unusually high HFI constants found by us for the Pt(III) compounds in the  $\text{K}_2\text{PtX}_6$  matrix can result from the substantial contribution of the  $6s$  orbital to the hybrid orbital on which an unpaired electron is localized (cf. [19]).

Let us consider possible routes of  $\text{Pt}^{3+}$  formation during the mechanical activation of Pt(IV) salts. This reaction can be performed by the homolytic cleavage of the Pt-Cl bond according to Eq. (I) or (for the combined grinding of the  $\text{K}_2\text{PtX}_6$  and  $\text{K}_2\text{PtX}_4$  salts) by the electron transfer in the  $\text{Pt}^{4+}-\text{Pt}^{2+}$  redox pair. Two facts allow us to exclude the last possibility. First, it is probable  $\text{Pt}^{3+}$  accumulation upon  $\text{K}_2\text{PtCl}_6$  grinding in the absence of  $\text{K}_2\text{PtCl}_4$  or other reducing agent can only occur due to Pt-Cl bond homolysis. Second, when  $\text{K}_2\text{PtCl}_6$  and  $\text{K}_2\text{PtBr}_4$  are milled together, for the reaction occurred through the electron transfer in the  $\text{Pt}^{4+}-$

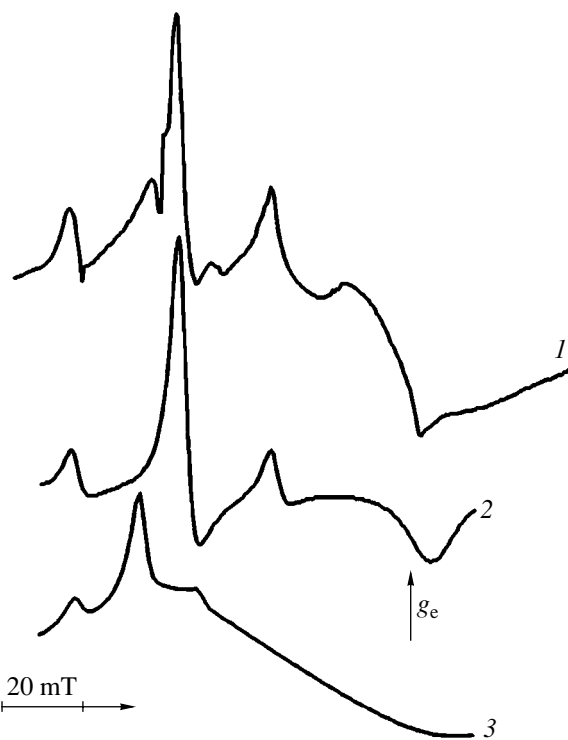


**Fig. 3.** ESR spectrum of the  $\text{Pt}^{3+}$  complexes produced by the mechanical treatment of the  $\text{K}_2\text{PtCl}_6 + \text{K}_2\text{PtBr}_4$  mixture: (1) experimental spectrum; (2) theoretical spectrum of Pt(III) chloride; and (3) theoretical spectrum of platinum(III) bromide at room temperature.

$\text{Pt}^{2+}$  pair the accumulation of equal amounts of platinum(III) chloride and bromide should be expected, which contradicts the experiment. The observed increase in the yield of Pt(III) upon the grinding of the Pt(IV) samples containing minor additives of Pt(II) can be explained by the ability of the latter to be oxidized with chlorine and thus shift equilibrium (I) to the right.

The  $\text{Pt}^{3+}$  concentration estimated from the ESR spectra monotonically increases with an increase in the mechanical energy dose absorbed by the powder and reaches the limit value of an order of  $1 \times 10^{18}$  species/g

Parameters of the ESR spectra of  $\text{Pt}^{3+}$  in some complexes described by the axially symmetric spin Hamiltonian

System	$g_{\perp}$	$g_{\parallel}$	$A_{\perp} \times 10^4, \text{ cm}^{-1}$	$A_{\parallel} \times 10^4, \text{ cm}^{-1}$	Literature
$\text{Pt}^{3+}$ in $\text{PtCl}_4$	2.18	1.98	6*	14*	[18]
$\text{Pt}^{3+}$ in $\text{Al}_2\text{O}_3$	2.328	2.011	—	—	[19]
$\text{Pt}^{3+}$ in $\text{BaTiO}_3$	2.459	1.950	135	0	[20]
$\text{Pt}^{3+}$ in $\text{K}_2\text{PtCl}_6$	2.371**	1.983**	500**	$<65^{**}$	This work
	2.385***	2.000***	511***	$0 \pm 35^{***}$	
$\text{Pt}^{3+}$ in $\text{K}_2\text{PtBr}_6$	2.45	1.95	317	$<420$	"

\* Hyperfine splitting constant, mT.

\*\* Room temperature.

\*\*\* 77 K.

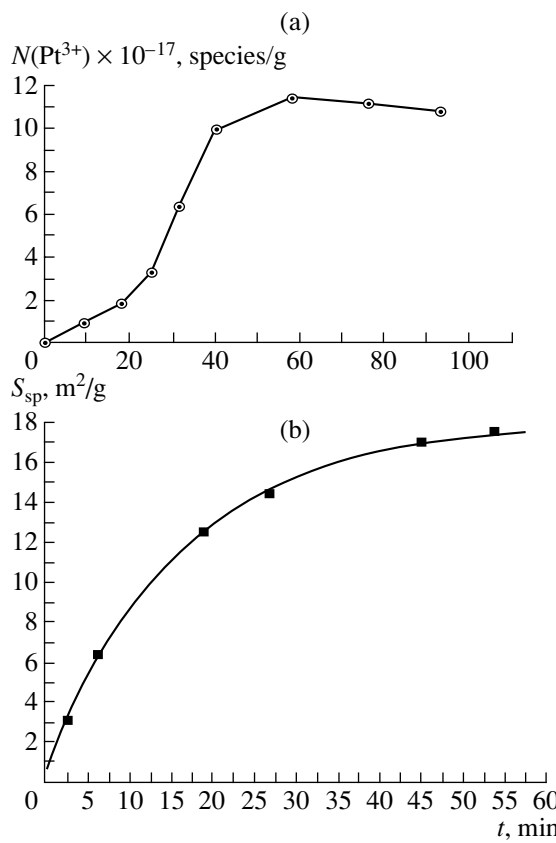


**Fig. 4.** Plots of the (a) amount of the  $\text{Pt}^{3+}$  complexes and (b) specific surface area of the  $\text{K}_2\text{PtCl}_6$  salt vs. duration of treatment.

(Fig. 4a).<sup>2</sup> The specific surface area of  $\text{K}_2\text{PtCl}_6$  increases in parallel with the amount of paramagnetic platinum. This function looks like a curve with saturation and can be described by the equation (Fig. 4b)

$$S_{\text{sp}} = S_0 + \alpha(1 - \exp(-\eta_s D_{\text{sp}})), \quad (2)$$

where  $S_0 = 0.7 \text{ m}^2/\text{g}$  is the specific surface area of the initial  $\text{Pt}(\text{IV})$ ,  $\alpha = (17.3 \pm 0.3) \text{ m}^2/\text{g}$ ,  $\eta_s = (0.06 \pm 0.01) \text{ g}/\text{J}$  is the constant characterizing the efficiency of new surface formation, and  $D_{\text{sp}}$  is the specific dose of the absorbed mechanical energy. Note that the maximum rate of accumulation of the paramagnetic species is observed after  $\sim 30$  min of the treatment when the specific surface area almost reaches its limiting value. This is obviously due to the fact that first the supplied energy is predominantly consumed for the formation of the new surface.

The intensity of ESR signals corresponding to the  $\text{Pt}^{3+}$  ions decreases with time, and a singlet with  $g = 2.000$  and  $\Delta H = 3 \text{ mT}$  appears and grows. However, its

<sup>2</sup> The concentration was measured immediately after the 1-h treatment of  $\text{K}_2\text{PtCl}_6$  with an additive of 15 mol %  $\text{K}_2\text{PtCl}_4$ . The yield of  $\text{Pt}(\text{III})$  upon the treatment of  $\text{K}_2\text{PtCl}_6$  without  $\text{K}_2\text{PtCl}_4$  additives under similar conditions is  $2 \times 10^{17}$  species/g.

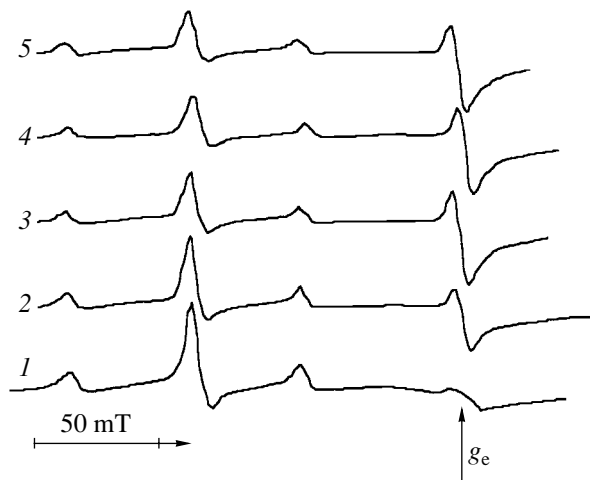
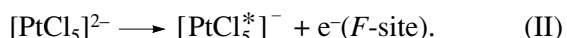


**Fig. 5.** ESR spectrum of the  $\text{Pt}^{3+}$  complexes produced by the mechanical treatment of the  $\text{K}_2\text{PtCl}_6 + \text{K}_2\text{PtCl}_4$  mixture detected after (1) 1, (2) 14, (3) 134, (4) 157, and (5) 189 h of treatment. Room temperature.

integral intensity remains much lower than that of the signal from the initial  $\text{Pt}(\text{III})$  (Fig. 5). The intensity of the  $\text{Pt}^{3+}$  signal can decrease for the following reasons: the disproportionation of  $\text{Pt}^{3+}$ , the formation of diamagnetic dimers of  $\text{Pt}^{2+}$ , and electron transfer from  $\text{Pt}^{3+}$  to some acceptor to form a diamagnetic  $\text{Pt}^{4+}$  species. Structural defects of the crystalline lattice, air oxygen, and other species can play the role of an electron acceptor. Based on the low mobility in the solid, we can exclude the first two possibilities. Taking into account the absence of an appropriate reducing agent in the system ( $\text{Pt}^{2+}$  does not suit this purpose because when an electron transfers from it,  $\text{Pt}^{3+}$  is formed again), we exclude the third possibility. We have the last one: the transfer of an electron from  $\text{Pt}^{3+}$  and the formation of the  $\text{Pt}(\text{IV})$  complex. We do not know what lattice defects stabilize this electron<sup>3</sup> but, by analogy with data for alkaline-halogen crystal [14], we can assume that their role can be played, in a particular case, by anionic vacancies bearing an effective positive charge. In addition to this analogy, the assumption is based on the appearance of paramagnetic sites with the  $g$ -factor characteristic of an electron captured by an anionic vacancy. Taking into account that the mobility in the solid is complicated by diffusion, the stoichiometric consequence of this reaction should be the formation of a  $\text{Pt}(\text{IV})$  complex anion with the coordination vacancy and, thus, the point defect in the form of a single-charge anion in the lattice of the  $\text{Pt}(\text{IV})$  salt



<sup>3</sup> We do not consider the electron transfer to air oxygen because the ESR spectrum does not contain the characteristic signal from the superoxide anion.

Electron transfer in reaction (II) to the site of localization of structural defects capable of accepting it can most likely proceed by the "relay" mechanism through the adjacent Pt(IV) complex anions with the intermediate formation of Pt(III).

The concentration of paramagnetic sites with  $g = 2.000$  in time passes through a maximum (Fig. 5). In the considered case, the role of the sink of defects of the  $F$  site type can also be played by Pt(III): the reduction of the latter by a free electron should result in the formation of Pt(II). In other words, despite the low mobility and relatively low concentration of the  $\text{Pt}^{3+}$  ions, a rather efficient diffusion-forbidden disproportionation of Pt(III) to Pt(II) and Pt(IV) can be expected in the solid  $\text{K}_2\text{PtCl}_6$  matrix.

The simultaneous occurrence of reaction (II) evidently implies that the free energy of the  $[\text{PtCl}_5^*]^-$  state and electron stabilized by the structural defect (presumably,  $F$  site) is lower than the corresponding value for Pt(III). Taking into account the electron affinity of the chlorine atom, we can assume that the observed mechanically activated homolytic cleavage of the Pt–Cl bond occurs in parallel with the heterolysis of this bond to form  $[\text{PtCl}_5^*]^-$  and an interstitial chloride ion. The point defect of the lattice in the form of the singly charged  $[\text{PtCl}_5^*]^-$  anion has an effective positive charge and is a Lewis acid site. The paramagnetic probe method using stable nitroxyl radicals as donating adsorbates is convenient for the identification and estimation of the concentration of Lewis acid sites on the solid surface [21–25]. We found that, when 2,2,6,6-tetramethylpiperidin-1-oxyl ( $0.18 \mu\text{mol}/\text{m}^2$ ) was supported on the surface ( $S_{\text{sp}} = 18 \text{ m}^2/\text{g}$ ) of the mechanically treated  $\text{K}_2\text{PtCl}_6$  salt, the ESR spectrum exhibited two signals from the nitroxyl radical along with the signal from  $\text{Pt}^{3+}$  (Fig. 6). The broad signal (signal A, Fig. 6) consists of three components with the anisotropic HFI tensor on the  $^{14}\text{N}$  nucleus and corresponds to radicals with low rotational mobility (cf. [21–24]). The apparent value of the anisotropic HFI constant  $A'_{zz}$  determined as a half-distance between the external extremes is usually used [21–24] as a parameter for the description of delayed spectra of adsorbed radicals. For signal A this parameter is equal to 33.1 Oe. In addition to signal A, the spectrum contains a triplet corresponding to radicals with a higher rotational mobility (Fig. 6, signal B). The addition of new portions of TEMPO increases the intensity of signal B, whereas the intensity of signal A remains virtually unchanged.

The results qualitatively agree with data on the adsorption of nitroxyl radicals on the alumina [22–25] and magnesium chloride [26] surfaces: TEMPO is first adsorbed on stronger acceptor sites (signal A). This state is characterized by the hindered mobility of the adsorbed radical and, correspondingly, a higher value

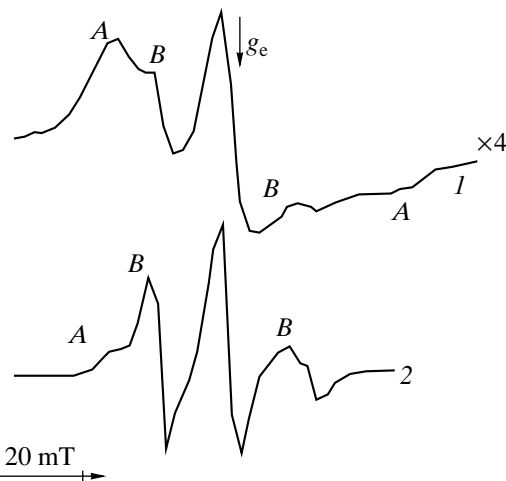


Fig. 6. Typical room-temperature spectra of TEMPO supported on the mechanically activated  $\text{K}_2\text{PtCl}_6$  salt surface. Curve 2 was obtained at a higher concentration of TEMPO compared to that for curve 1.

of the  $A'_{zz}$  parameter. In our case,  $A'_{zz}$  is much lower than that determined for TEMPO adsorbed on magnesium chloride [26] (38.6 Oe) and alumina [23] (39.0 Oe). This evidently implies that the acid sites generated by the mechanical treatment of  $\text{K}_2\text{PtCl}_6$  produce a less stable complex with the radical. After all acceptor sites capable of reacting with the radical are occupied, the addition of new portions of TEMPO results in its less stable binding with the surface [22] (physical adsorption). For physically adsorbed radicals the correlation time of rotational motion is much shorter resulting in the situation when their ESR signal approaches signal B in the spectrum of the radical in a solution. The estimation from the ESR spectra of the amount of Lewis acid sites (LAS) on the surface of a 1-g sample, under the condition that the {TEMPO–acceptor site of the surface} complex has the 1-to-1 stoichiometry [21] gives  $N_{\text{LAS}} \approx 3 \mu\text{mol}/\text{g}$ . The obtained  $N_{\text{LAS}}$  value can likely be considered as the lower limit of the LAS concentration: not all acceptor sites of the surface can be sterically accessible to the stable radical. Compare  $N_{\text{LAS}}$  with the number of complex anions on the surface of 1 g of the salt ( $N_{\text{Pt}}$ ). The estimation of  $N_{\text{Pt}}$  from the lattice parameter [27] of  $\text{K}_2\text{PtCl}_6$   $a = 9.78 \times 10^{-10} \text{ m}$  and the specific surface areas gives  $N_{\text{Pt}} \approx 60 \mu\text{mol}/\text{g}$ .

Let us consider a possible nature of acceptor sites of the surface of the mechanically activated  $\text{K}_2\text{PtCl}_6$  salt. Anionic vacancies and their associates with an effective positive charge along with the coordinatively unsaturated  $[\text{PtCl}_5^*]^-$  complexes can play the role of such states can. However, it is difficult to imagine that more than 5% of the activated salt surface is occupied by anionic vacancies: in the case of the platinum salt, the anion consists of seven atoms and is much larger than

that in alkaline halides. In addition, a stronger binding with TEMPO and, hence, a higher  $A'_{zz}$  parameter should be expected for the anionic vacancy bearing in our case the effective positive charge  $2+$ . It is most likely that the coordinatively unsaturated Pt(IV) complexes make the main contribution to LAS observed by us. Note that the amount of these complexes is at least twice as large as the amount of paramagnetic platinum.

In conclusion, we would like to note that supporting TEMPO does not result in the exchange broadening of the signal from  $\text{Pt}^{3+}$ : the parameters and intensity of the signal remain unchanged. These values also remained unchanged after purging a freshly treated sample with gaseous chlorine capable of oxidizing Pt(III). We conclude that the  $\text{Pt}^{3+}$  species detected by the ESR method are localized inside the crystals or, which is more probable<sup>4</sup> on the surface of grain interfaces, which are inaccessible to adsorption from the gas phase.

## CONCLUSIONS

Thus, the mechanical treatment of the solid-phase  $\text{K}_2\text{PtX}_6$  ( $\text{X} = \text{Cl}, \text{Br}$ ) salts leads to the formation of metastable and, hence, potentially reactive species, i.e., Pt(III) complexes, and, probably, coordinatively unsaturated Pt(IV) complexes. Such species with coordination vacancies are often considered as key intermediates of several catalytic processes [29]. A search for these compounds with different organic substrates and their study are underway in our laboratories.

## ACKNOWLEDGMENTS

This work was supported by INTAS (grant no. 97-1874).

## REFERENCES

1. Shilov, A.E., *Activation of Saturated Hydrocarbons by Transition Metal Complexes*, Reidel: Dordrecht, 1984.
2. Luinstra, G.A., Wang, L., Stahl, S.S., Labinger, J.A., and Bercaw, J.E., *J. Organomet. Chem.*, 1995, vol. 504, p. 75.
3. Hutson, A.C., Lin, M., Basickes, N., and Sen, A., *J. Organomet. Chem.*, 1995, vol. 504, p. 69.
4. Mitchenko, S.A. and Zamashchikov, V.V., *Kinet. Katal.*, 1989, vol. 30, no. 2, p. 297.
5. Mitchenko, S.A., Zamashchikov, V.V., and Shubin, F.F., *Kinet. Katal.*, 1993, vol. 34, no. 3, p. 479.

<sup>4</sup> We proceed from the fact that the point defects of the structure are predominantly localized in the near-surface crystalline layers, whereas two-dimensional defects are localized in the crystallite depth (see, for example, [28]).

6. Mitchenko, S.A., Ananikov, V.P., Beletskaya, I.P., and Ustynguk, Yu.A., *Mendeleev Commun.*, 1997, no. 4, p. 130.
7. Tret'yakov, V.P. and Osetskii, A.N., *Kinet. Katal.*, 1982, vol. 23, no. 5, p. 1126.
8. Subbotina, I.R., Shelimov, B.N., and Kazanskii, V.B., *Kinet. Katal.*, 1998, vol. 39, no. 1, p. 87.
9. Butyagin, P.Yu., *Kinet. Katal.*, 1987, vol. 28, no. 1, p. 5.
10. Buyanov, R.A., Zolotovskii, B.P., and Molchanov, V.V., *Sib. Khim. Zh.*, 1992, no. 2, p. 5.
11. Butyagin, P.Yu., *Usp. Khim.*, 1994, vol. 63, no. 12, p. 1031.
12. Mitchenko, S.A., Khomutov, E.V., Kovalenko, V.V., Popov, A.F., and Beletskaya, I.P., *Mendeleev Commun.*, 1999, no. 5, p. 171.
13. *Sintez kompleksnykh soedinenii metallov platinovoi gruppy. Spravochnik* (Synthesis of the Complex Compounds of Platinum Group Metals, a Handbook), Chernyaev, I.I., Ed., Moscow: Nauka, 1964.
14. Mitchenko, S.A., Dadali, Yu.V., and Kovalenko, V.V., *Zh. Org. Khim.*, 1998, vol. 34, no. 9, p. 1293.
15. Thiele, J. and Peter, W., *Chem. Ber.*, 1905, vol. 38, p. 3842.
16. Zefirov, N.S., Zhdankin, V.V., Makhon'kova, G.V., Dan'kov, Yu.V., and Koz'min, A.S., *J. Org. Chem.*, 1985, vol. 50, no. 11, p. 1872.
17. Heinike, G., *Tribochemistry*, Berlin: Akademie, 1984, p. 169.
18. Shubochkin, L.K., Gushchin, V.I., Larin, G.M., and Kolosov, V.A., *Zh. Neorg. Khim.*, 1974, vol. 19, no. 2, p. 460.
19. Geschwind, S. and Remeika, J.P., *J. Appl. Phys.*, 1962, vol. 33, no. 2, p. 370.
20. Simanek, E., Sroubek, Z., Zdansky, K., Kaczer, J., and Novak, L., *Phys. Status Solidi*, 1966, vol. 14, no. 3, p. 333.
21. Larin, G.M., *Zh. Neorg. Khim.*, 1997, vol. 42, no. 7, p. 1163.
22. Golubev, V.B., Lunina, E.V., and Selivanovskii, A.K., *Usp. Khim.*, 1981, vol. 50, no. 5, p. 793.
23. Fionov, A.V., Zaitseva, I.M., Kharlanov, A.N., and Lunina, E.V., *Kinet. Katal.*, 1997, vol. 38, no. 1, p. 155.
24. Lunina, E.V., Zacharova, M.N., Markayan, G.L., and Fionov, A.V., *Colloids Surf.*, 1996, vol. 115, p. 195.
25. Lunina, E.V., *Appl. Spectrosc.*, 1996, vol. 50, p. 1413.
26. Mikenas, T.B., Vitus, E.N., Zakharov, V.A., Bedilo, A.F., and Volodin, A.M., *Kinet. Katal.*, 1997, vol. 38, no. 1, p. 150.
27. Kukina, G.A., *Zh. Strukt. Khim.*, 1962, vol. 3, no. 1, p. 108.
28. Gol'dberg, E.L. and Eremin, A.F., *Izv. Sib. Otd. Akad. Nauk SSSR, Ser. Khim. Nauk.*, 1985, vol. 6, no. 17, p. 16.
29. Rudakov, E.S., *Zh. Fiz. Khim.*, 1987, vol. 61, no. 2, p. 289.